Drag and Stability of Objects in a Yield Stress Fluid

Laurent Jossic and Albert Magnin
Laboratoire de Rhéologie, B. P. 53, 38041 Grenoble Cedex 9, France
Université Joseph Fourier Grenoble 1, Institut National Polytechnique de Grenoble, CNRS UMR 5520, France

The drag force exerted on objects in a yield stress fluid was measured when the velocities become infinitely slow. In these quasi-static conditions, yield stress effects are predominant. Particular care was paid to determining the yield stress and checking interface conditions when characterizing these fluids from a rheometric standpoint. Drag coefficients could then be determined for interesting objects of various shapes. The important role of fluid-object interface effects was also highlighted. On the basis of these results, a stability criterion is proposed for the object in the fluid, to estimate the yield stress needed to balance buoyancy forces.

Introduction

In many industrial applications such as concrete or food, it is important to be able to predict the stability of solid objects in a viscoplastic suspending phase. To do this, it is necessary to control the basic mechanisms of the phenomena governing drag at very low velocities, as well as the stability of the isolated objects. And, yet, in spite of the many industrial challenges involved, knowledge of this subject is limited. Chhabra (1993) made an exhaustive summary of the results given in the literature concerning the behavior of isolated objects in viscoplastic fluids. Most of these results concern spheres, and the case of nonspherical objects has received little attention (Boardman and Whitmore, 1960, 1962; Rae, 1962; Brooks and Whitmore, 1968). Even though some disagreement remains concerning spheres, the results obtained by Atapattu et al. (1995), Beaulne and Mitsoulis (1997), and Blackery and Mitsoulis (1997) converge and provide new data. In contrast, knowledge concerning nonspherical objects is still just as limited as before.

The first objective of this study is to provide an experimental estimate of the drag force exerted on an isolated object moving at a very low prescribed velocity, in quasi static conditions, in a viscoplastic fluid. In contrast to sedimentation experiments, the prescribed velocity removes any uncertainty concerning stress distribution on the surface of the object. On the basis of these results, an evaluation of the stability criterion is proposed, using drag coefficients obtained when the velocity tends towards zero. These results were obtained by paying special attention to important aspects, which were not usually taken into account in previous studies. An experimental setup is used to move objects at very low prescribed velocities to obtain stress levels of the order of magnitude of the yield stress. This is situated in the quasi-static domain, which has been explored very little in previous experiments. Phenomena in this field are governed by yield stress. Nonthixotropic viscoplastic fluids were characterized in detail in the low shear rate domain close to that involved in the experiment. Any possible slip at the surface of the rheometric devices was monitored. Precise and controlled measurement of the yield stress removed one of the main uncertainties in determining the stability criterion linked to the exact value of the yield stress. The roughness length scales of the objects were also monitored. It appears that conditions at the fluid-object interface play a major role with respect to the value of the stability criterion. This aspect has never been discussed in the literature. The role of interface roughness may be linked to slip at the wall observed in rheometric tests. Lastly, the effect of orientation on drag coefficients and object stability will also be analyzed.

Correspondence concerning this article should be addressed to A. Magnin.

Theoretical Approach

An object moving in a viscoplastic fluid at very low velocity creates stresses in its immediate vicinity of the order of the yield stress τ_0. The drag force F_d exerted upon it may there-

fore be expressed as a dimensionless quantity by the product $A.\tau_0$ in which A represents the frontal area of the object in question along a plane perpendicular to the flow, that is, the surface opposing the flow. Hence, the drag coefficient

$$C_d^* = \frac{F_d}{A.\tau_0} \tag{1}$$

This expression is only meaningful in the field of infinitely low velocities where inertia and viscous effects are negligible in comparison with yield stress effects.

The behavior of the viscoplastic fluids used in this experiment may be modeled one-dimensionally by the Herschel-Bulkley equation

$$\begin{cases} \tau = \tau_0 + K\dot{\gamma}^n & \text{if } \dot{\gamma} \neq 0 \\ \tau \leq \tau_0 & \text{if } \dot{\gamma} = 0 \end{cases} \tag{2}$$

This equation imposes the following expressions for the Reynolds and Bingham numbers, respectively

$$Re = \frac{\rho l^n U^{2-n}}{K} \tag{3}$$

$$Bi = \frac{\tau_0}{K(U/l)^n} \tag{4}$$

ρ represents the density of the fluid. In the case of an object moving in an infinite medium, l represents the characteristic length scale of the object; this is defined more precisely below.

The ratio of yield stress effects to gravity effects is represented by the dimensionless number Y

$$Y = \frac{\tau_0}{gl\Delta\rho} \tag{5}$$

where l is the characteristic dimension of the object in question and $\Delta\rho$ is the difference in density between the fluid and the object. The smallest value of this number, for which the object is immobile, is referred to as the stability criterion: $Y_{\max}$. By making the buoyancy force and drag force due to the yield stress equal, $l = V/A$ in which V is the volume of the object. However, in order to calculate the stability criterion, objects of different shapes were considered to be equivalent to spheres of equal volume. This definition, which involves taking a sphere as reference, means that it is possible to determine how well the stability criterion is evaluated for a random object on the basis of the value obtained in the case of a sphere. Moreover, it has the advantage of enabling different shapes to be compared at constant volume.

The buoyancy force exerted on the objects can thus be written

$$F_b = \frac{\pi}{6} g\Delta\rho d_e^3 \tag{6}$$

with $d_e = (6V/\pi)^{1/3}$ the diameter of a sphere of the same volume. At very low velocities, this force is balanced by a drag force due to the yield stress, which is in theory independent of the velocity. This can be expressed in the form

$$F_d = C\tau_0 \frac{\pi d_e^2}{4} \tag{7}$$

C is a dimensionless coefficient. Hence, it is possible to derive an experimental evaluation of the stability criterion for the object

$$Y_{\max} = \frac{\tau_0}{gd_e\Delta\rho} = \frac{2}{3C} \tag{8}$$

In the case of the sphere, $Y_{\max}$ may be calculated by considering that the tangential stresses on the surface of the sphere are all equal to τ_0 (Andres, 1961). Thus, $Y_{\max} \approx 0.212$. It will be shown below that this calculation hypothesis is too high, and that the value obtained for $Y_{\max}$ is therefore overestimated.

Experimental Setup

The experimental setup designed for the test is shown in Figure 1. The assembly for moving the reservoir consists of a plate guided by two vertical columns and two motors. The two motors have complementary velocity ranges. They can be used to move the plate at a constant speed between 10^{-2} and 10^{-6} m·s^{-1}. Given the objects and the gels used, the Bingham numbers involved during the experiments are between 1 and 10. The Reynolds numbers are between 10^{-1} and 10^{-8}.

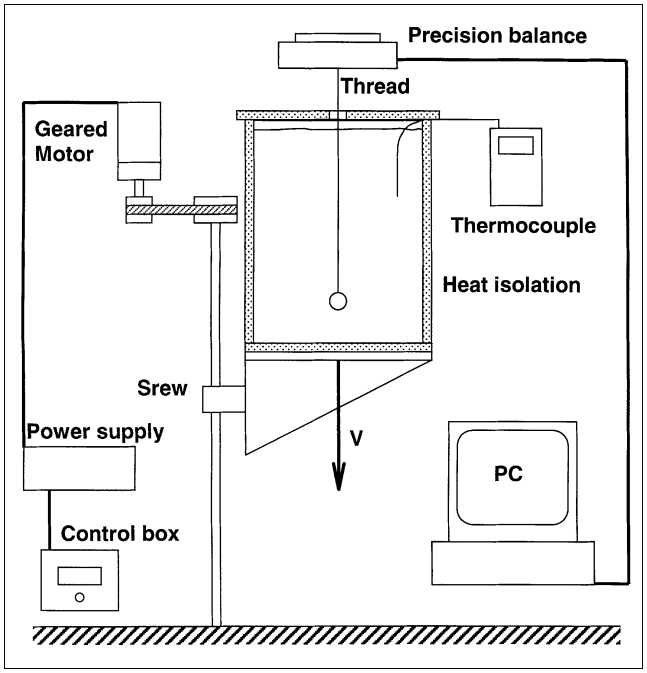

Figure 1. Experimental setup for measuring drag force at prescribed velocity.

Table 1. Shape of Objects Used*

	Surface	Dimensions (mm)
Sphere	Smooth	$d = 20$
	Rough	$d = 22$
Disc	Smooth	$d = 35.4$; $h = 1.2$
$h/d = 0.02$	Rough	$d = 35.7$; $h = 2.7$
Cylinder	Smooth	$d = 35$; $h = 5$
$h/d = 0.14$	Rough	$d = 36.5$; $h = 6.5$
		$d = 37.5$; $h = 7.2$
Cylinder	Smooth	$d = h = 20$
$h/d = 1$	Rough	$d = 21.1$; $h = 21.4$
Cylinder	Smooth	$d = 10$; $h = 50$
$h/d = 5$	Rough	$d = 11.5$; $h = 51.5$
Cube	Smooth	$a = 20$
	Rough	$a = 22$
Cone	Smooth	$d = 35.2$; $h = 17.6$
$\alpha = 90°$	Rough	$d = 35.4$; $h = 17.7$

*d: diameter, h: height, a: edge, α: top angle.

The object is suspended on a Precisa 400M precision balance with a capacity of 400 g and a precision of 1 mg, by means of a nylon thread 0.05 mm in diameter. The balance is connected to a computer, used for data acquisition.

Ordinary-shaped objects were considered. The dimensions of those used in the experiments are listed in Table 1. They were all made of stainless steel. The roughness of the "smooth" objects was evaluated, and found to be of the order of 1 μm or less. In the case of the sphere it was of the order of 0.01 μm. The "rough" objects were obtained by gluing sand to them. They had a roughness of the order of 250 μm.

The reservoir has a diameter $D = 160$ mm, and its height is $H = 300$ mm. Typically, the ratio between reservoir diameter and characteristic size of the object is of the order of 5. Given the yield stresses and velocities involved, the objects may be considered to be in an infinite medium (Atapattu et al., 1990, 1995; Beaulne and Mitsoulis, 1997; Blackery and Mitsoulis, 1997). The fluid is sufficiently deep for a steady regime to be obtained.

The experimental setup was validated using a Newtonian fluid with a sphere. After subtracting the drag force exerted along the immersed thread, the experimental drag force differs from the theoretical value by less than 6%. This value is less than the experimental uncertainties. If the fluid is viscoplastic and nonthixotropic, drag effects on the thread are less marked, at least when the velocities are low. It is then possible, as a first approximation, to consider that the thread and object are subjected to a yield stress. The ratio of drag forces is then equal to the ratio of surface areas, and it is therefore important for the surface area of the thread to be as small as possible in comparison with that of the object.

Of all the objects studied, the one for which disturbance due to the thread is most important is that for which the drag force is least, that is, the disc. When this is held by a 50 μm diameter thread, and the length immersed in the fluid is 20 cm, the drag force of the thread represents only 2.8% of the disc drag force.

The extraneous friction of the thread was measured experimentally. It is indeed low in comparison with the drag of the object and lower than the calculated value, probably because the fluid slips on the thread. Slip effects are examined below.

It became apparent during the different tests that free surface effects are negligible. As surface tension and gravity effects are greater than viscous effects, the thread is not coated by the viscoplastic fluid during the experiments. Moreover, no capillarity force that could have added an extraneous force to the drag was recorded.

End effects are disturbances to measurements linked with the bottom of the reservoir and free surface. These effects were estimated. In the case of the sphere, they are felt at distances equivalent to about one sphere diameter from the bottom of the reservoir and about five sphere diameters from the free surface. In the case of the other objects, the diameter can be replaced by the characteristic length scale of the object. The measurements were performed in the section where these effects are negligible.

Material and Rheometry

Various Carbopol 940 gels manufactured by Goodrich were used. These are aqueous gels obtained by mixing a polymer in water. The mixture is neutralized by adding soda. During neutralization, the gel becomes viscoplastic. The yield stress value can be adjusted as a function of concentration and pH. The material obtained in this way is transparent, viscoplastic, and nonthixotropic (Magnin and Piau, 1990), and its properties are stable in time.

The yield stress values were carefully determined by means of prescribed shear rate rheometry using a cone-plate device. Shear rates as low as 5×10^{-5} s^{-1} could be obtained. The rheometer used for the experiment was a Carrimed Weissenberg rheogoniometer. Evaporation effects were controlled during the longer tests. Gel slip against the tool surfaces was controlled by using "rough" tools (Magnin and Piau, 1987, 1990).

Figure 2 represents the flow curves for the various gels used, showing shear stress vs. shear rate under steady conditions. These curves were modeled by a Herschel-Bulkley law (Eq. 2). The model parameters for each gel are listed in Table 2.

It is vital to determine the yield stress accurately, and, to do this, rheometric measurements were made right down to very low shear rate values. A clear stress plateau was thus obtained, enabling the yield stress to be determined precisely

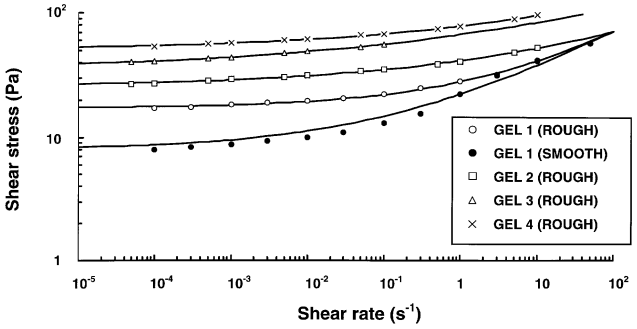

Figure 2. Gel flow curves.

For gel 1, the influence of the surface roughness of the rheometric tools is shown.

Table 2. Rheometric Characteristics of Gels Used*

	τ_0 (Pa)	K (Pa·s^n)	n
Gel 1	17.3	16.6	0.32
Gel 2	35.8	31	0.19
Gel 3	25.9	15.5	0.23
Gel 4	51.4	26.8	0.22

*Values obtained with "rough" tools.

by extrapolation. This has not always been the case in previous studies (Chhabra, 1993). The yield stresses obtained by extrapolation were confirmed by additional measurements using the vane test method (Liddell and Boger, 1996), with the above conditions and strict monitoring of slip and strain fields in the sample (Magnin and Piau, 1987, 1990).

In the case of gel 1, measurements were performed with "smooth" and "rough" tools (Figure 2). In the case of the "smooth" surfaces, with a roughness value of less than a micron, slip could be displayed at the fluid-tool interface (Magnin and Piau, 1987, 1990). The apparent stress values are lower when slip occurs. The error in yield stress value is of the order of a factor of 2 if slip at the wall is not considered. These measurements clearly illustrate the effects of slip at the wall depending on interface conditions.

Experimental Results

The following experimental protocol was adopted. The first stage involves rating the balance when it is empty. The second involves measuring the mass of the object suspended in air. The object is then immersed in the fluid, far enough from the bottom, for the end effects to be negligible. The plate is then moved at constant velocity to measure the drag force.

The change in signal during the tests at different velocities with a "smooth" sphere and "rough" sphere is shown in Figure 3. At the beginning, when the object is static in a viscoplastic fluid, it is subjected to buoyancy forces and to a residual force, connected with the yield stress, produced during immersion. The forces increase during the transient regime, which is of the order of twice the characteristic length scale of the object, irrespective of velocity and roughness. This stage corresponds to elastic strain of the material up to the point of flow, that is, the point at which it exceeds the critical strain, and to proximity effects at the bottom of the reservoir.

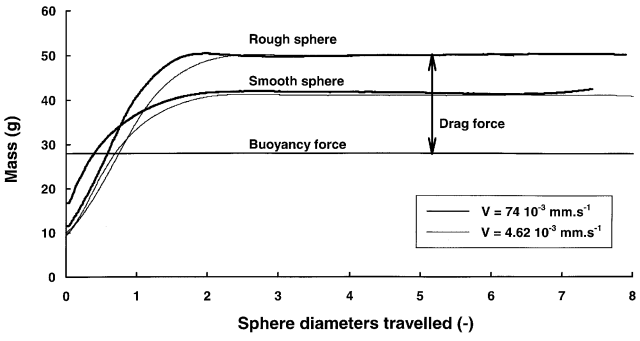

Figure 3. Change in signal at different velocities for "smooth" and "rough" spheres.

Table 3. Experimental Results*

	Position	Surface	$C_d^* = F_d/A \cdot \tau_0$	Y_{max}
Sphere	—	Smooth	6.7	0.088
		Rough	11.5	0.062
Disc $h/d = 0, 02$	Horizontal	Smooth	27.7	0.077
		Rough	30.6	0.054
Cylinder $h/d = 0, 14$	Horizontal	Smooth	16.7	0.078
		Rough	17.9	0.067
	Vertical	Smooth	12.3	0.019
		Rough	12	0.023
Cylinder $h/d = 1$	Horizontal	Smooth	8.3	0.082
		Rough	10.7	0.064
	Vertical	Smooth	9.4	0.093
		Rough	27.8	0.063
Cylinder $h/d = 5$	Horizontal	Smooth	9.5	0.042
		Rough	11	0.038
	Vertical	Smooth	17	0.150
		Rough	32	0.075
Cube	Horizontal	Smooth	6.5	0.125
		Rough	6.7	0.061
	Vertical	Smooth	10.5	0.044
		Rough	9.8	0.048
Cone	—	Smooth	10.1	0.026
		Rough	9.9	0.027

*See text for definition of orientation.

The signal then stabilizes. The force measured does not depend on the velocity when this is low, but is a function of the yield stress, surface roughness, shape, and orientation of the object.

The third area corresponds to a disturbance of the forces on approaching the free surface. The distance from which these effects occur is independent of the velocity and in the case of the sphere is of the order of five sphere diameters.

Discussion

The drag coefficients and stability criteria measured in the test are given in Table 3. In the case of the disc and cylinders, the vertical position is that for which the axis of symmetry is vertical and parallel to the direction of flow. The cube is vertical when the straight line connecting two opposite corners is vertical. The horizontal position corresponds to the case where the upper and lower faces are perpendicular to the flow direction. A single position was considered for the cones, with the base perpendicular to the flow direction.

Measurements were taken for each object over a range of velocities running from 10^{-6} to 10^{-3} m·s^{-1}. Figure 3 represents the total force measured in the case of a "smooth" sphere and a "rough" sphere. It appears that the force during steady conditions is independent of the velocity, when the velocity tends towards very low values. This conclusion was reached for the different shapes. The stresses created by displacement are of the order of magnitude of the yield stress and independent of the velocity. They correspond to the plateau of the flow curve, where stress is independent of shear rate. Drag force is therefore independent of displacement velocity and governed by yield stress. This justifies the use of

yield stress to express drag force in dimensionless form. It is also a good reason for evaluating the stability criterion corresponding to zero displacement velocity from drag force measurements in quasi-static conditions. Lastly, it should be noted that the reproducibility of the measurements is distinctly higher than those of the sedimentation measurements of Atapattu et al. (1995) and Hariharaputhiran et al. (1998).

Tests were performed on the same object with "smooth" and "rough" surfaces placed in gels with different yield stresses (Table 1). The forces measured are in the ratio of the yield stresses. The drag force is therefore a linear function of the yield stress. The differences obtained with regard to the value of the stability criterion are within the uncertainty of measurement.

An examination of Table 3 and Figures 3–7 shows that the drag forces measured on the "smooth" objects are of the same order of magnitude or less than those measured on the "rough" objects. The largest differences are observed in the case of the sphere and cylinders with a slenderness factor of 1 and 5 in the vertical position. These differences are examined in greater detail below. However, it may be assumed immediately that the slip observed during rheometric characterization also occurred in flow around the obstacles. This aspect has never been taken into account in previous studies. A special study should therefore be conducted to determine the influence of roughness length scale on drag force. The results obtained with "rough" surfaces are in theory the closest to those of wall adherence, which correspond to the theoretical studies. They will therefore be given closer attention in this study.

The Carbopol gels are suspensions of microgels (Hariharaputhiran et al., 1998; B.F. Goodrich, 1997). The typical length scale of microgels is the micrometer. When the length scale of the surface roughness is greater than that of the microgels, slip does not occur at the wall.

The case of the cylinders is particularly interesting as it enables a single geometric parameter to be varied, in order to observe its effect. Figures 4 and 5 show the change in drag coefficient C_d^* as a function of slenderness factor for horizontal and vertical positions, respectively.

In a horizontal position (Figure 4), C_d^* is independent of slenderness from $h/d = 1$ onwards. Beyond this ratio, the drag force is proportional to the frontal area. The minimum slenderness for a horizontal cylinder to be considered infinite in a viscoplastic fluid appears to be a few units. In the case of Newtonian fluids, this value is at least of the order of 10. This difference may be explained by the fact that the stresses set up by the movement of an object do not propagate as far in a viscoplastic fluid as in a Newtonian one. When the ratio h/d tends towards zero, C_d^* appears to vary inversely to h/d. The lateral surfaces play an increasingly important role. The drag force tends to become proportional to the lateral surface area.

In a horizontal position, the drag coefficients obtained with "smooth" surfaces are slightly lower than those obtained with "rough" surfaces. The differences due to roughness are slight in comparison with those recorded in vertical position.

In a vertical position (Figure 5), when h/d tends towards zero, the drag coefficient tends towards a constant value. The drag force is then proportional to the frontal area and independent of h. When h/d increases, C_d^* varies linearly with h/d. The drag force then varies in proportion to the product $A.h/d$, that is, to the lateral surface area. For a given diameter, the drag force therefore varies linearly with the length of the cylinder. As in the case of the horizontal cylinder, it appears that the case of the infinite cylinder is reached once the ratio h/d reaches a few units.

Roughness plays no role when slenderness tends towards zero. In this case, C_d^* is determined by the geometry of the object, that is, the frontal area, and not by the surface state. Beyond $h/d = 1$, the differences observed between "smooth" and "rough" objects grow as the lateral surface area increases in relation to the frontal area. These differences may be explained by the fact that the gel slips against the surface of the objects. This assumption is all the more justified as the shear rates involved are small. Slip therefore appears to occur mainly on the lateral surfaces. The influence of roughness on drag coefficient therefore depends on orientation.

To examine the influence of object shape, C_d^* is represented as a function of the ratio between lateral surface area and frontal area (Figure 6). The surface area of the object projected on to a vertical plane is referred to as the lateral surface area S_{lat}. In this way it is possible to assess the influence of yield stress on the front and lateral surfaces.

In the case of S_{lat}/A ratios less than a value of the order of 4, C_d^* is relatively constant and of the order of 10 for "rough" objects. In the case of "smooth" objects, it becomes $C_d^* \approx 9$. The drag force for these objects depends on the frontal area and relatively little on the shape. Beyond $S_{\text{lat}}/A \approx 4$, C_d^* increases significantly with the ratio S_{lat}/A. The drag force for these objects depends on the lateral surface area.

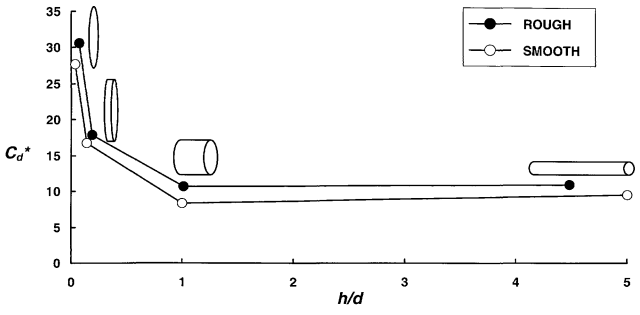

Figure 4. Change in drag coefficient C_d^* of a horizontal cylinder as a function of slenderness.

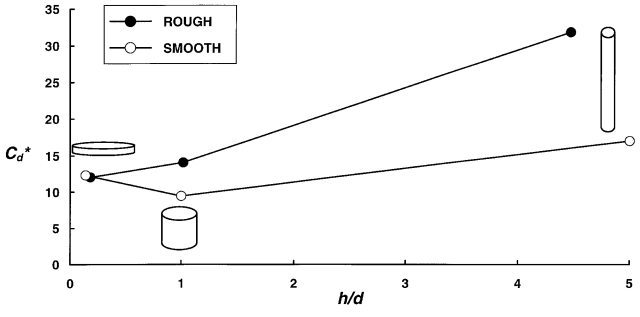

Figure 5. Change in drag coefficient C_d^* of a vertical cylinder as a function of slenderness.

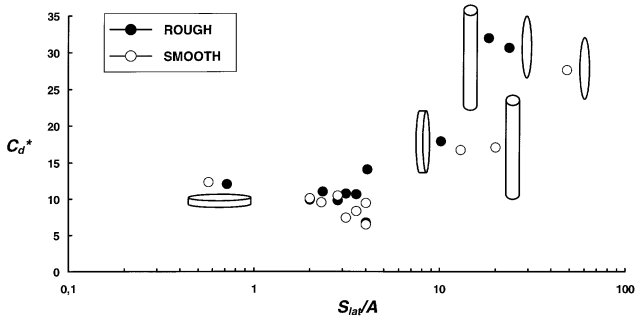

Figure 6. Change in drag coefficient C_d^* as a function of ratio S_{lat}/A.

For a given object, C_d^* therefore depends on its orientation, especially when the object is not spheroidal. Thus, in the case of the "rough" cylinder with a slenderness factor of 5, C_d^* varies by 65% between the horizontal and vertical positions. In the case of the cylinder with a slenderness factor of 1, it is only 24%.

The values obtained for S_{lat}/A less than 4 are lower than those proposed by Brooks and Whitmore (1968): $C_d^* = 16.7$. This difference may be due to uncertainties concerning the yield stress. Indeed, it should be noted that this result was obtained with a clay suspension that probably has a thixotropic behavior. In this case, the yield stress depends on the shear history of the fluid, and the measurements were performed after the object had been moved at a velocity of 7 $cm \cdot s^{-1}$ and then suddenly stopped. This method may result in indeterminacy in the initial stress distribution around the object. By moving the object at a very low velocity, this indeterminacy is overcome and the loading method is controlled. Moreover, the yield stress was not determined in the shear rate field corresponding to the experiments. It was obtained by extrapolation from high shear rates.

The role of object-yield stress fluid interface conditions demonstrated in the case of cylinders is found again to varying extents with the other objects. The differences in drag force between "smooth" and "rough" objects grow as lateral surface areas increase in relation to frontal area. Slip at the wall appears to occur particularly on lateral surfaces.

Table 3 and Figure 7 can be used to classify the stability criteria obtained for the various objects according to their shape, surface state, and orientation. These criteria were defined by considering the various objects to be equivalent to spheres of the same volume (Eqs. 6–8). For a given volume, this graph can be used to determine the geometry and orientation requiring the lowest yield stress to achieve stability. It can also be used to evaluate the quality of the approximation assuming that the stability criterion for an object is the same as that for the sphere of equal volume.

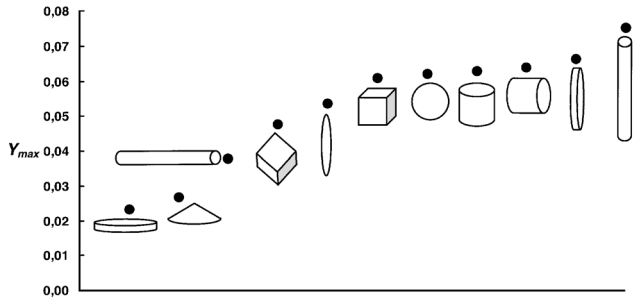

Figure 7. Stability criterion of "rough" objects as a function of their shape and orientation.

For a given object, regardless of roughness, the stability criterion value appears to be lowest in the position where the frontal area is greatest. The object's orientation therefore has an effect on its stability.

The various shapes are classified according to increasing values of Y_{max}, in the case of "rough" surfaces. A higher yield stress is required to keep a cylinder with a slenderness factor of 5 vertical than a cube of the same volume, when they have "smooth" surfaces. If the surfaces are "rough," a higher yield stress is required to stabilize the cube than the cylinder. The greatest differences between "smooth" and "rough" surfaces are obtained in the case of a cylinder with a slenderness factor of 5 (50%), a cube (51%), and a sphere (41%). This value partly explains the considerable scatter, which is around an order of magnitude, between the values proposed in the literature (Chhabra, 1993). Most of the experimental results proposed so far were obtained with "smooth" spheres. Hence, there is the considerable differences in relation to the values obtained by numerical calculation. Using the stability criterion of a sphere to predict the stability of another object may produce values that differ by a factor of up to 2, especially in the case of a horizontal disc or cone.

Conclusions

The results presented above provide new information on the stability of commonly shaped objects (sphere, cube, cylinder, disc, and so on) in yield stress fluids. The drag coefficient in quasi-static conditions and a stability criterion were estimated for each shape. These results were obtained by carefully controlling the fundamental stability criteria. First of all, measurements were performed in the quasi-static domain, where inertia effects are negligible in comparison with yield stress effects. This domain has so far received very little experimental attention. The yield stress was also evaluated precisely. To do this, the yield stress fluid was characterized in the shear rate domain involved in quasi-static mode. Conditions at the fluid-object interface were also monitored. This parameter has never been taken into account in previous studies, yet it is one of the essential stability parameters. As these three parameters have never been monitored simultaneously so far, it is easy to explain why there is such a considerable scatter in the values found in the literature.

Using this approach, it is possible to suggest an estimate of the drag coefficient for various objects in a viscoplastic fluid. This drag coefficient is obtained by expressing the drag force in dimensionless form using the product of frontal area multiplied by yield stress. When the velocity becomes infinitely slow, the stresses set up in the fluid become independent of velocity and of the order of magnitude of the yield stress. Using the drag forces obtained in this way, it is possible to estimate the stability criterion corresponding to zero velocity. The stability criterion of a given object was determined by considering it to be equivalent to a sphere of the same vol-

ume. Using these values, it is then possible to determine the shapes and corresponding yield stresses for an object of given volume to be stabilized in a viscoplastic fluid. The drag coefficient and stability criterion values were discussed as a function of the shape of the objects, the ratio of lateral surface area to frontal area, their orientation and roughness. Major differences in stability criterion of as much as 50% could be recorded for some shapes, depending on whether the surface was "smooth" or "rough." These differences are probably caused by the fluid slipping at the wall of the "smooth" objects. This slip occurs mainly on the lateral surfaces, and, therefore, depends on the orientation of the object.

These new experimental data are especially interesting as data concerning nonspherical objects are so far extremely fragmented. It would be interesting to explore the effect of roughness on the stability criterion in greater depth.

Notation

a = cube edge, m
A = frontal area, m^2
$Bi = \tau_0/K(U/l)^n$ = Bingham number
C = coefficient
$C_d^* = F_d/A \cdot \tau_0$ = drag coefficient
d = object diameter, m
D = reservoir diameter, m
F = force, N
g = gravity, $m \cdot s^{-2}$
h = object height, m
H = reservoir height, m
K = consistency, $Pa \cdot s^n$
l = characteristic length scale of object, m
n = flow index
$Re = \rho U^{2-n} l^n/K$ = Reynolds number
S = surface area, m^2
U = velocity, $m \cdot s^{-1}$
V = volume, m^3
$Y = \tau_0/gd_e\Delta\rho$ = stability criterion
α = top angle, deg
τ_0 = yield stress, Pa
τ = shear stress, Pa
$\dot{\gamma}$ = shear rate, s^{-1}
ρ = density, $kg \cdot m^{-3}$
$\Delta\rho$ = difference in density between fluid and object, $kg \cdot m^{-3}$

Subscripts

b = buoyancy
d = drag
e = equivalent
lat = lateral

Literature Cited

Andres, U. Ts., "Equilibrium and Motion of Spheres in a Viscoplastic Liquid," *Sov. Phys. Doklady (USA)*, **5**, 723 (1961).

Atapattu, D. D., R. P. Chhabra, and P. H. T. Uhlherr, "Creeping Motion in Herschel-Bulkley Fluids: Flow Field and Drag," *J. Non-Newtonian Fluid Mech.*, **59**, 245 (1995).

Atapattu, D. D., R. P. Chhabra, and P. H. T. Uhlherr, "Wall Effect for Spheres Falling at Small Reynolds Number in a Viscoplastic Medium," *J. Non-Newtonian Fluid Mech.*, **38**, 31 (1990).

Barnes, H. A., "A Review of the Slip (Wall Depletion) of Polymer Solutions, Emulsions and Particle Suspensions in Viscometers: Its Cause, Character and Cure," *J. Non-Newtonian Fluid Mech.*, **56**, 221 (1995).

Beaulne, M., and E. Mitsoulis, "Creeping Motion of a Sphere in Tubes Filled with Herschel-Bulkley Fluids," *J. Non-Newtonian Fluid Mech.*, **72**, 55 (1997).

B. F. Goodrich Literature, *Carbopol Resins Handbook*, Cleveland, OH (1997).

Blackery, J., and E. Mitsoulis, "Creeping Motion of a Sphere in Tubes Filled with a Bingham Plastic Material," *J. Non-Newtonian Fluid Mech.*, **70**, 59 (1997).

Boardman, G., and R. L. Whitmore, "Response to Rae D," *Nature*, **194**, 272, (April 1962).

Boardman, G. and R. L. Whitmore, "Yield Stress Exerted on a Body Immersed in a Bingham Fluid," *Nature*, **187**, 50 (July 1960).

Brooks, G. F., and R. L. Whitmore, "The Static Drag on Bodies in Bingham Plastics," *Rheologica Acta*, **7**, 188 (1968).

Chhabra, R. P., *Bubbles, Drops and Particles in Non-Newtonian Fluids*, CRC Press, London (1993).

Hariharaputhiran, M., R. S. Subramanian, G. A. Campbell, and R. P. Chhabra, "The Settling of Spheres in a Viscoplastic Fluid," *J. Non-Newtonian Fluid Mech.*, **79**, 87 (1998).

Liddell, P. V., and D. V. Boger, "Yield Stress Measurements with the Vane," *J. Non-Newtonian Fluid Mech.*, **63**, 235 (1996).

Magnin, A., and J.-M. Piau, "Shear Rheometry of Fluids with a Yield Stress," *J. Non-Newtonian Fluid Mech.*, **23**, 91 (1987).

Magnin, A., and J.-M. Piau, "Cone and Plate Rheometry of Yield Stress Fluids. Study of an Aqueous Gel," *J. Non-Newtonian Fluid Mech.*, **36**, 85 (1990).

Rae, D. "Yield Stress Exerted on a Body Immersed in a Bingham Fluid," *Nature*, **194**, 272 (Apr., 1962).

Manuscript received Sept. 25, 2000, and revision received May 23, 2001.